Generation of an extreme ultraviolet supercontinuum with a multicycle chirped laser and a static electric field*

Zhang Gang-Tai(张刚台)[a)†], Bai Ting-Ting(白婷婷)[b)], and Zhang Mei-Guang(张美光)[a)]

[a)] *Department of Physics and Information Technology, Baoji University of Arts and Sciences, Baoji* 721016, *China*
[b)] *Department of Mathematics, Baoji University of Arts and Sciences, Baoji* 721013, *China*

(Received 10 April 2012; revised manuscript received 17 May 2012)

We theoretically present a method for generating an ultrabroad extreme ultraviolet (XUV) supercontinuum by using the combination of a multicycle chirped laser and a static electric field. At a low laser intensity, the spectral cutoff is extended to the 495th order harmonic, and the bandwidth of the supercontinuum spectrum is broadened to 535 eV. At a high laser intensity, the harmonic cutoff is enlarged to the 667th order, and a supercontinuum covering a bandwidth of 1035 eV is generated. In these two cases, the long quantum path is removed, and the short quantum path is selected. Especially for the relatively high laser intensity, an isolated 23-attosecond pulse with a bandwidth of about 170.6 eV is directly obtained. Finally, we also analyze the influences of the chirp parameter and the duration of the chirped pulse as well as the static field strength on the supercontinuum.

Keywords: high-order harmonic, attosecond pulse generation, supercontinuum, combined field

PACS: 42.65.Ky, 32.80.Rm, 42.65.Re **DOI:** 10.1088/1674-1056/21/11/114209

1. Introduction

The appearance and development of isolated attosecond (as) pulses has paved a way for studying and operating basic ultrafast electronic processes in atoms and molecules with unprecedented accuracy and resolution.[1−3] So far, high-order harmonic generation (HHG) is the most advanced method to produce a single attosecond pulse experimentally. The physical mechanism of the HHG can be well understood by using a semiclassical three-step model.[4] According to the model, the electron first tunnels through the barrier formed by the atomic potential and the laser field, then it oscillates almost freely in the laser field, and finally it may return to the ground state by recombining with the parent ion. During the recombination, a photon with energy equal to the ionization potential plus the kinetic energy of the recombining electron is emitted. The above process is repeated every half optical cycle of the driving pulse, which results in the generation of an attosecond pulse train (APT) with a periodicity equal to half of the optical cycle.

In the practical application, since a single attosecond pulse is more useful in the pump–probe experiment, how to produce an isolated attosecond pulse has drawn a great deal of attention. It has been shown that an isolated attosecond pulse can be generated with a few-cycle laser pulse[1,2,5] or a polarization gating technique.[3] An isolated 80-as pulse, which is currently the shortest attosecond pulse, was realized in a recent experiment.[6] However, the durations of the single attosecond pulses are still far longer than the natural time scale of electron motion in atoms, i.e., 24 as. Therefore, it is necessary to broaden the bandwidth of the isolated attosecond pulse and push the duration to shorter time. Very recently, it has been proposed that a two-color field can broaden the bandwidth of the supercontinuum and be used to obtain an isolated short attosecond pulse. Zeng *et al.*[7] showed that a 148-eV supercontinuum can be generated by a two-color field, then an isolated 65-as pulse was directly created. Lan *et al.*[8] proposed that a synthesized two-color field can coherently control the electron dynamics, and showed that this method can not only broaden the attosecond pulse bandwidth and reduce the harmonic chirp, but also produce a close-to-Fourier-limited 80-as pulse. Moreover, they also proposed that an ionization gating, which can be achieved

*Project supported by the Science Foundation of Baoji University of Arts and Sciences, China (Grant Nos. ZK10122, ZK11061, ZK11135, ZK11060, and ZK1032) and the Natural Science Foundation of the Education Committee of Shaanxi Province, China (Grant No. 2010JK405).

†Corresponding author. E-mail: gtzhang79@163.com

© 2012 Chinese Physical Society and IOP Publishing Ltd

with a few-cycle laser pulse in combination with its second harmonic, can generate an isolated attosecond electron wave packet and an isolated broadband 135-as extreme ultraviolet (XUV) pulse.[9] An alternative method for generating a broadband attosecond pulse is controlling the quantum paths. In the single-atom response, the quantum path control can be realized by using a two-color field,[10−14] an APT,[15] or a ultraviolet (UV) pulse.[16,17] In the real scenario of the HHG, a full description of the propagation of the driving field and the high harmonics through the gas medium at the macroscopic level is required. It has been reported that the phase matching in the propagation plays an important role in the HHG.[18,19] By carefully adjusting the gas pressure or the position of the laser focus, one can realize the phase matching conditions for either a short quantum path or a long one, and then a single quantum path can be macroscopically selected. Lan *et al.*[20] showed that only the short quantum path can be selected after the propagation through the helium gas and an isolated 130-as pulse is obtained. In addition, they also studied the HHG of the asymmetric molecules and demonstrated that the selection of the long quantum path can be achieved by placing the gas jet before the laser focus. They demonstrated the generation of an isolated 95-as pulse with a 47-eV bandwidth.[21] Dai *et al.*[22] theoretically investigated the macroscopic effects of the harmonic generation by a two-color field and showed that a specific range of harmonics can be enhanced dramatically by adjusting the time delay and the relative intensity between the fundamental and the frequency-doubled laser pulses.

With the introduction of a chirp, many schemes with a chirp form are employed to extend the harmonic cutoff and broaden the bandwidth of the XUV supercontinnum, from which a broadband isolated attosecond pulse can be obtained. Carrera *et al.*[23] extended the HHG cutoff and created an isolated 108-as pulse via the coherent control of an intense few-cycle chirped laser pulse. Wu *et al.*[24] realized the extension of high-order harmonics and generated an isolated 38-as pulse by using intense few-cycle linearly chirped laser pulses. Xiang *et al.*[25] theoretically demonstrated the extension of the HHG cutoff and the generation of an isolated 10-as pulse with phase compensation by using a chirped few-cycle laser and a static electric field. Li *et al.*[26] directly obtained an isolated 26-as pulse by using an intense few-cycle chirped laser and its high-order harmonic pulses. Xu *et al.*[27] proved the extension of harmonic cutoff in a multicycle chirped pulse combined with a chirp-free pulse. Feng *et al.*[28] generated an isolated sub-40-as pulse using two-color laser pulses with the combined chirp effects.

HHG in the presence of a static electric field has been extensively investigated.[29−34] It has been shown that a static electric field is a very useful means to control the high harmonic emission rate,[29] the maximum harmonic photon energy,[30−33] and the polarization properties of harmonics.[34] Although the effects of the single chirped pulse and the chirped pulse in combination with the static electric field have been investigated,[23−25] few studies have been reported for the combination of the chirped pulse and the static electric field in the multicycle regime. In this paper, we investigate the HHG of a model neon atom in a multicycle chirped laser and a static electric field. The numerical results show that the extensions of both the harmonic cutoff and the XUV supercontinuum can be achieved by using this method. Furthermore, the electron trajectories for HHG are significantly modulated in the presence of the static electric field, as a result, only the short quantum path is selected to contribute to the harmonic generation. When the intensity of the chirped pulse is relatively high, by superposing some proper continuous harmonics, an isolated attosecond pulse as short as 23 as is directly obtained. In particular, the influences of the chirp parameter and the duration of the chirped pulse as well as the static field strength on the supercontinuum are investigated.

2. Model and methods

In our simulation, the HHG spectrum and attosecond pulse generation can be studied by numerically solving the one-dimensional time-dependent Schrödinger equation with the splitting operator method.[35] The simulation method is based on the single active-electron approximation and has been widely employed in the HHG simulation. The harmonic spectrum is obtained by Fourier transforming the time-dependent dipole acceleration for a model atom. The temporal profiles of the attosecond pulses can be generated by simply performing the inverse Fourier transformations of the XUV supercontinua in different spectral regions. In our calculation, the soft Coulomb potential $V(x) = -1/\sqrt{x^2 + a^2}$ is adopted, where $a = 0.817$ is chosen to match the ionization energy 0.792 a.u. of a real Ne atom. The driving pulse consists of a 10 fs/800 nm chirped laser pulse and a

static electric field, which is given as

$$E(t) = E_0 f_0(t) \cos[\omega_0 t + \delta(t)] + E_1, \quad (1)$$

where E_0 and E_1 are the amplitudes of the chirped pulse and the static electric field, respectively, ω_0 and $\delta(t)$ are the corresponding frequency and time profile of the carrier envelope phase (CEP) of the laser field, $f_0(t) = \exp[-2\ln(2)(t/\tau_0)^2]$ denotes the Gauss envelope of the laser field, and $\tau_0 = 10$ fs is the pulse duration of the full width at half maximum (FWHM). The form of the CEP is $\delta(t) = -\beta \tanh[(t - t_0)/\tau]$, where parameters β, t_0, and τ are used to control the chirp form. In this work, t_0 and τ are chosen to be 0 a.u. and 200 a.u., respectively.

3. Results and discussion

To verify our scheme, we first investigate the HHG process according to the semiclassical three-step mode. Here, the intensities of the chirped pulse and the static electric field are 4.0×10^{14} W/cm^2 and 2.8×10^{13} W/cm^2, respectively, and $\beta = 6.25$ is adopted. Figure 1(a) shows the electric field of the 10 fs/800 nm chirped pulse alone. Figure 1(b) shows the corresponding dependence of the harmonic order on the ionization and the emission times. From Fig. 1(b), we can see that the electrons are mainly ionized near the peaks (labelled by P_1, P_2, and P_3) of the electric field. The highest order harmonic is at the 241st order due to the electrons ionized near peak P_2, and the second-highest order harmonic is at the 134th order due to the electrons ionized near peak P_3, whereas the electrons ionized near peak P_1 are mainly attributed to the harmonics lower than the 129th order. Therefore, only the harmonics from the 134th order to the 241st order become continuous, corresponding to a supetcontinuum with a bandwidth of 166 eV. For the continuous harmonics, each order harmonic is generated only through two electron trajectories. The trajectory with an earlier ionization time but a later emission time is called the long trajectory, and the other trajectory with a later ionization time but an earlier emission time is called the short trajectory. As the harmonic order increases, the emission time for the short trajectory increases, and that for the long trajectory decreases, and these two emission times are equal for the highest-order harmonic. This result indicates that the harmonics in the second plateau are not emitted in phase, and the harmonics in the cutoff region are only emitted at the same time. Thereby, the superposition of several plateau harmonics will lead to an attosecond pulse train with two bursts in each optical cycle of the driving pulse. Only when the single quantum path is picked out, an isolated attosecond pulse can be produced.

When a static electric field is added to the chirped laser pulse, the electronic dynamics in the HHG process is significantly modulated. In order to substantiate this fact, we perform the classical trajectory simulation of the electrons in the chirped pulse combined with the static electric field. Figure 1(c) shows the combined electric field. Figure 1(d) shows the corresponding dependence of the harmonic order on the ionization and the emission times. As shown in Figs. 1(c) and 1(d), the electron is no longer ionized near the peak of the driving field, instead it is ionized from -1.32 o.c. to -0.68 o.c. and from 0.62 o.c. to 1.27 o.c. and forms two dominant ionization events labeled by R_2 and R_3. Though there is an ionization event taking place (labeled by R_1), R_1 only contributes to the harmonics below the 84th order. The highest order harmonic is at the 486th order, which is ascribed to the electron ionized at -1.3 o.c. and recombined at 0.38 o.c. The second-highest order harmonic is at the 144th order, which is ascribed to the electron ionized at 0.93 o.c. and recombined at 2.05 o.c. Compared with the case of the chirped pulse alone, since the highest order of the harmonics is greatly increased and the second-highest order of the harmonics is increased a little, the frequency difference between them (i.e., between peaks R_2 and R_3) becomes much larger than that in Fig. 1(b). The enlarged frequency difference explains why an ultrabroad XUV supercontinuum spectrum can be formed in the field shown in Fig. 1(c). Furthermore, we notice that for the supercontinuum origined from the ionization event R_2, only the short trajectory contributes to each harmonic, which implies that the harmonics higher than the 144th order are almost locked in phase and emit simultaneously with one single quantum path contribution. Considering all the results above, we can conclude that under the modulation of the static electric field, the harmonic cutoff is extended to the 486th order harmonic, and a spuercontinuum with a bandwidth of about 530 eV is generated, which can support isolated short attosecond pulse generation.

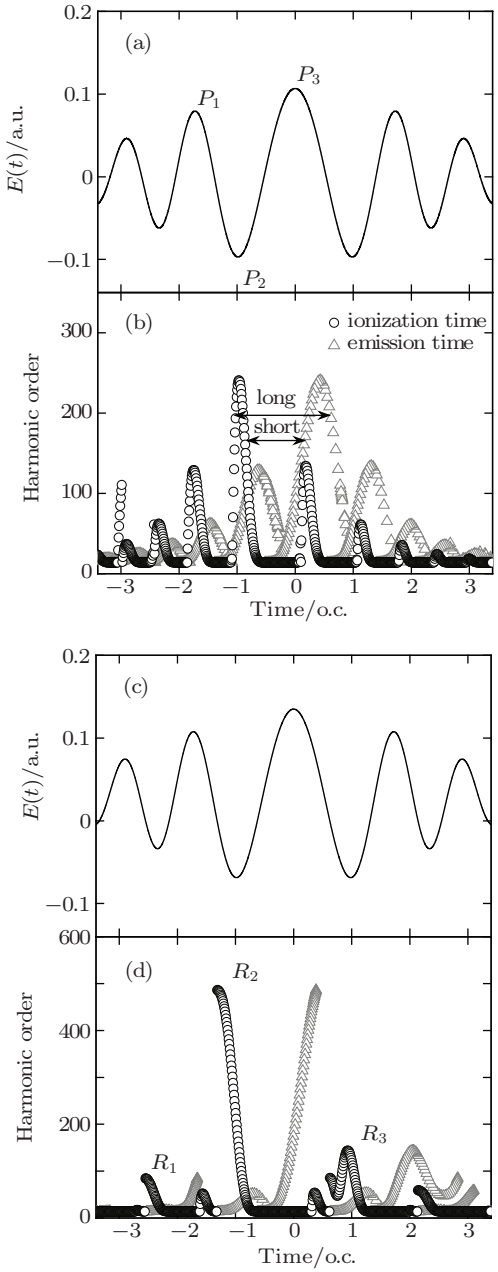


Fig. 1. (a) Electric field of the 10 fs/800 nm chirped pulse alone. (b) Dependence of the harmonic order on the ionization and the emission times in the field shown in panel (a). (c) Electric field of the 10 fs/800 nm chirped pulse in combination with the static electric field. (d) Dependence of the harmonic order on the ionization and the emission times in the field shown in panel (c). The intensities of the chirped pulse and the static electric field are 4.0×10^{14} W/cm^2 and 2.8×10^{13} W/cm^2, respectively, and $\beta = 6.25$ is adopted. The o.c. represents the optical cycle throughout this paper.

To confirm the classical theory predictions above, we investigate the HHG spectrum using the full quantum calculation. All the parameters are the same as those in Fig. 1. Figure 2 presents the harmonic spectra in the fields mentioned above. As shown by the solid line in Fig. 2(a), the harmonic spectrum shows an irregular structure, and the spectrum cutoff is only at the 63rd order harmonic, and only a few order harmonics in the cutoff region become continuous. With the introduction of the chirp, the harmonic spectrum shows a different structure in comparison with that in the chirp-free pulse case. As shown in Fig. 2(a), the harmonic spectrum (dotted line) exhibits a two-plateau structure, the cutoff in the first plateau is at the 134th order harmonic, and the cutoff in the second plateau is significantly extended to the 241st order harmonic. Additionally, the harmonics higher than the 134th order become continuous, thus an XUV supercontinuum is formed in the second plateau. However, the supercontinuum shows a deep modulation structure, which is due to the interference of the long and the short quantum paths. As is well known, the supercontinuum with a modulation structure is not beneficial to the production of a single attosecond pulse. By applying a static electric field to the chirped pulse, the harmonic spectrum shows a distinct structure, as shown in Fig. 2(c). The spectrum cutoff is remarkably extended to the 495th order harmonic, and the spectrum above the 150th order becomes very regular and continuous, namely, an ultrabroad XUV supercontinuum spectrum is generated. Moreover, the modulation in the supercontinuum is largely reduced, implying that one single quantum path is selected. In order to understand the spectrum structure, we investigate the emission time of the harmonics with the wavelet transform method.[36] The result is presented in Fig. 2(d). For comparison, the time-frequency distribution of the HHG spectrum in the chirped pulse alone case is also shown in Fig. 2(b). Clearly, there are three peaks contributing to the harmonics, which are labeled by R_1, R_2, and R_3, respectively. The maximum harmonic orders of R_1, R_2, and R_3 are approximately at the 90th, the 495th, and the 150th, respectively. Among these three peaks, the intensity of R_1 is the weakest, the intensities of R_2 and R_3 are nearly comparable. In addition, the harmonics above the 150th order only originate from the contribution of R_2, forming an ultrabroad XUV supercontinuum with a bandwidth of about 535 eV. Compared with the case of using only the chirped pulse, the bandwidth of the supercontinuum in the combined field is much broader. For the harmonics below the 150th order, the interference among R_1, R_2, and R_3 results in an irregular spectrum structure, which is shown in Fig. 2(c). It is worthwhile to note that for peak R_2, the long quantum path (the negative-slope branch) is completely eliminated, and only the short quan-

tum path (the positive-slope branch) exists, which indicates that the broadband supercontinuum is contributed only by the short path harmonics, i.e., the harmonics for R_2 are almost phase-locked. Since the phase-locked harmonics cover a large frequency range, an isolated short attosecond pulse can be generated. All results above are in good agreement with those obtained by the three-step model shown in Fig. 1(d).

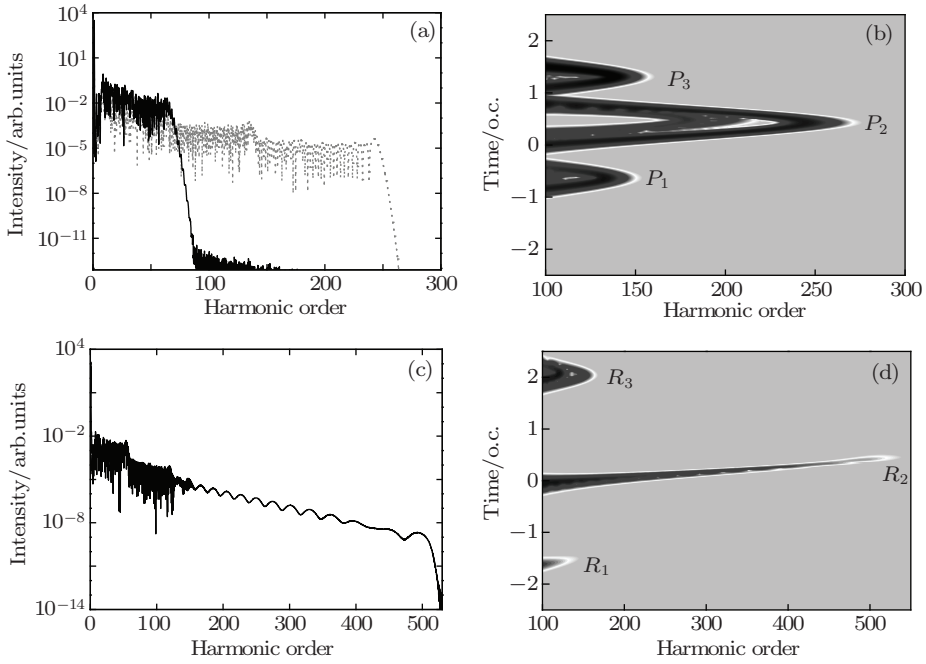


Fig. 2. (a) Harmonic spectra in the chirp-free (solid line) and the chirped (dotted line) pulses. (b) The time-frequency distribution of the HHG spectrum corresponding to the dotted line in panel (a). (c) Harmonic spectrum in the chirped pulse in combination with the static electric field. (d) The time-frequency of the HHG spectrum corresponding to panel (c). All the parameters are the same as those in Fig. 1.

In the following, we investigate attosecond pulse generation. The intensity of the chirped pulse is $I_0 = 4.0\times10^{14}$ W/cm^2. For comparison, the inset in Fig. 3 shows the temporal profile of the attosecond pulse by superposing the harmonics from the 185th order to the 220th order in the chirped pulse alone case. As shown in this figure, two bursts of radiation with comparable intensities are generated in each optical cycle. This is because there are two quantum paths with different emission time and nearly equal contribution corresponding to the same harmonic shown in Fig. 2(b). Since the plateau harmonics are not emitted at the same time, the superposition of several plateau harmonics will result in an attosecond pulse train containing two pulses in every optical cycle. Such an attosecond pulse train is very difficult to be used in the pump–probe experiment or the measurement of ultrafast dynamic processes. Figure 3 presents the temporal profile of the attosecond pulse in the combined field. We choose 88 order harmonics from the 163th to the 251th, an isolated 38-as pulse with a bandwidth of about 136 eV is directly produced without any phase compensation, which is different from that shown in the inset of Fig. 3. We also notice that the main peak is accompanied by several subpeaks, whereas the intensity ratio between the strongest subpeak and the main peak is 0.36, so it can be ignored.

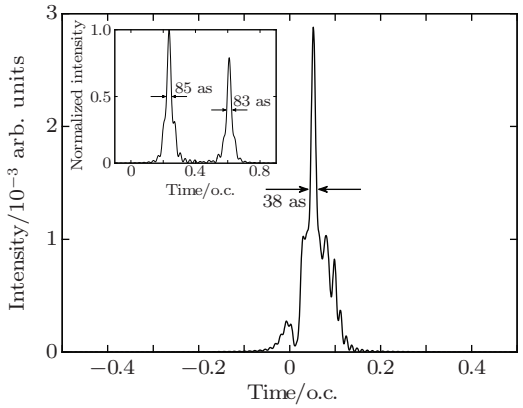


Fig. 3. The temporal profile of the attosecond pulse by superposing the harmonics from the 163th order to the 251th order. The inset shows the temporal profile of the attosecond pulse by superposing the harmonics from the 185th order to the 220th order in the chirped pulse alone case. The other parameters are the same as those in Fig. 1.

Now, we consider the case of the chirped pulse with an intensity of 6.0×10^{14} W/cm^2. The other parameters are the same as those in Fig. 1. The harmonic spectrum is shown in Fig. 4(a). As shown in this figure, the harmonic spectrum reveals two separated plateaus. The cutoff of the first plateau is at the 89th order harmonic, corresponding to the energy of 138 eV, and the second one is at the 667th order harmonic, corresponding the energy of 1035 eV.

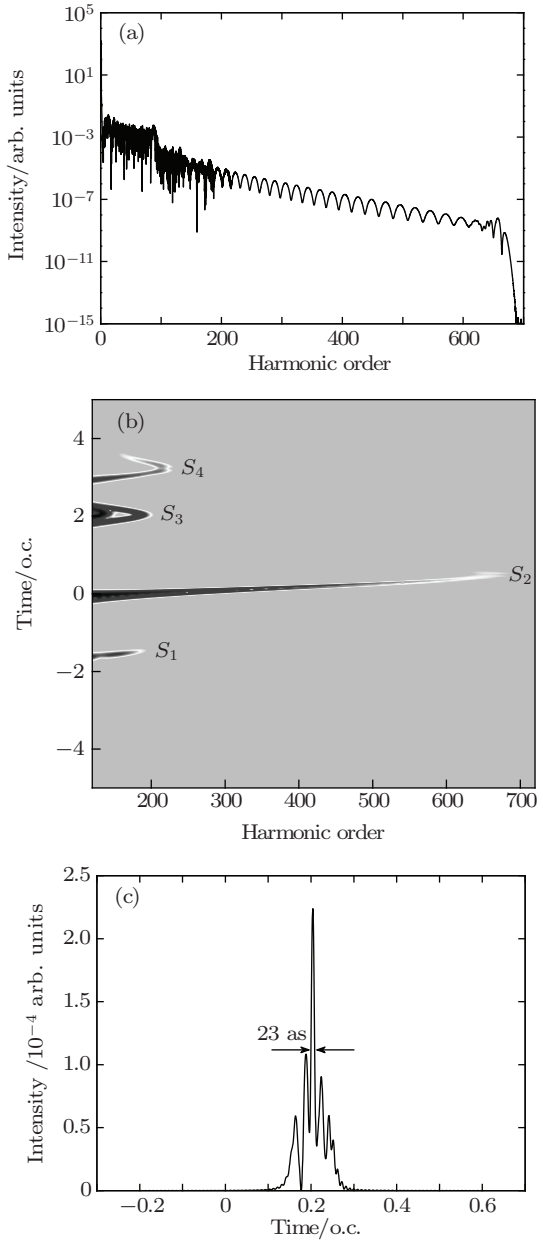


Fig. 4. (a) Harmonic spectrum in the combined field. (b) Time-frequency distribution of the HHG spectrum shown in panel (a). (c) Temporal profile of the attosecond pulse by synthesizing the harmonics from the 390th order to the 500th order. The intensity of the chirped pulse is 6.0×10^{14} W/cm^2. The other parameters are the same as those in Fig. 1.

Though the harmonic intensity of the second plateau is at least one magnitude lower than that of the first plateau, the spectrum is smooth and regularly modulated for the harmonics from the 219th order to the cutoff. Figure 4(b) shows the corresponding time-frequency distribution of the HHG in Fig. 4(a). It can be seen that there are four peaks (labeled by S_1, S_2, S_3, and S_4) contributing to the harmonic generation, and the maximum harmonic orders for S_1, S_2, S_3, and S_4 are about 145, 667, 179, and 219, respectively. For the harmonics below the 219th order, there are at least three quantum paths with different emission times contributing to the same harmonic, the interference of these quantum paths leads to an irregular spectral structure. For the harmonics above the 219th order, there is only one short quantum path (the positive-slope branch) contributing to the harmonic generation, which implies that the harmonics above the 219th order are almost emitted in phase. Thus a large number of harmonics emitted in phase are generated. This demonstrates a potential for producing an ultrashort isolated attosecond pulse. In order to check the above analysis, we investigate the attosecond pulse generation for this case. Figure 4(c) illustrates the single attosecond pulse generated by superposing the harmonics from the 390th order to the 500th order. As shown in this figure, the duration of this isolated attosecond pulse is about 23 as with a bandwidth of 170.6 eV, which is first smaller than the atomic unit of time (24 as) by directly filtering the HHG spectrum. The isolated 23-as pulse contains only 3.8 optical cycles of the central wavelength of 1.8 nm. Such a short isolated attosecond pulse will enable the detection and the control of the electronic dynamics inside atoms and molecules.

In the presence of the static electric field, by introducing a chirp form with a proper parameter to the fundamental laser pulse, we extend the harmonic cutoff and broaden the supercontinuum width. But we want to concretely know what is the effect of the chirp parameter β. For this purpose, we take the case with $I_0 = 4\times10^{14}$ W/cm^2 as an example to investigate the HHG processes in the combined field with different chirp parameter β by using the semiclassical three-step model. Figure 5(a) shows the dependences of the 1st and the 2nd cutoffs of the HHG on parameter β for the cases of two different durations. For the case of $\tau_0 = 10$ fs, as we increase β from 0 to 10, the 2nd cutoff of the HHG enlarges from 0 to 7.9, reaches the maximum value at $\beta = 7.9$, and finally decreases to the 438th order at $\beta = 10$; whereas the 1st cutoff

of the HHG has no significant change (from the 107th order to the 146th order). According to the definition of continuum spectrum in Ref. [7], i.e., the frequency difference between the highest and the second-highest cutoffs, in our method, the harmonic cutoff and the width of the supercontinuum reach the maxima at $\beta = 7.9$. The HHG spectrum for this parameter is presented by the black line in Fig. 5(b). We can find that the continuum spectrum is broadened to 475 order harmonics, corresponding to a supercontinuum with a bandwidth of about 737 eV. For the case of $\tau_0 = 20$ fs, a similar result is obtained, and a harmonic spectrum with a cutoff of 777 order and a supercontinuum with a bandwidth of 856 eV are obtained at $\beta = 8.5$, as shown by the gray line in Fig. 5(b). In addition, for the case of $I_0 = 6 \times 10^{14}$ W/cm^2, similar results can be obtained if the chirp parameter β changes from 0 to 10. In the case of $\tau_0 = 10$ fs, the 1st and the 2nd cutoffs of the spectrum are at approximately the 204th order and the 1014th order, respectively, at $\beta = 8.3$, which results in an ultrabroad XUV supercontinuum with a bandwidth of 1261 eV. In the case of $\tau_0 = 20$ fs, at $\beta = 9.1$, the spectral cutoff is extended to the 1290th order harmonic, and the supercontinuum ranges from the 296th order to the 1290th order, covering a bandwidth of 1542 eV. This unique property may offer an opportunity to produce an ultrashort isolated attosecond pulse by filtering a large number of harmonics emitted in phase.

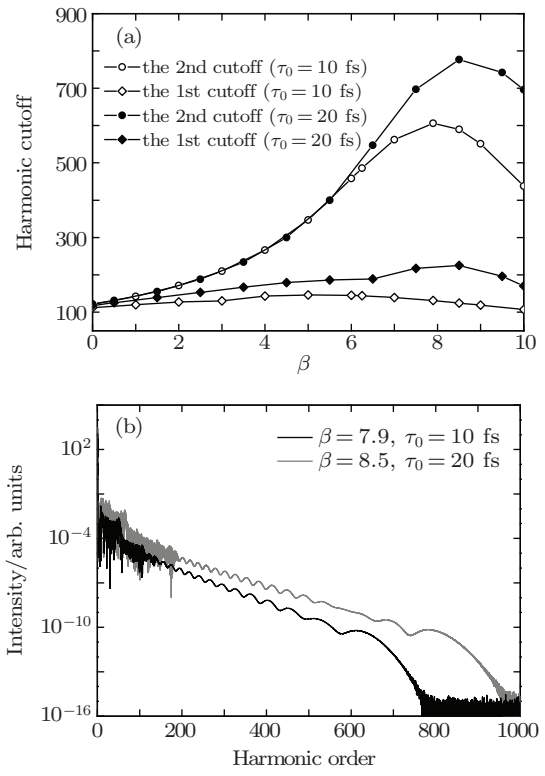


Fig. 5. (a) Dependences of the 1st and the 2nd cutoffs of the HHG on parameter β in the combined field for two different durations of 10 fs and 20 fs. (b) HHG spectra in the combined field. The other laser parameters are the same as those in Fig. 1.

Finally, we investigate the influences of the duration of the chirped pulse (τ_0) and the intensity of the static electric field (I_1) on the supercontinuum. The other parameters are the same as those in Fig. 1. Figure 6(a) presents the harmonic spectra for the cases with three different durations. As shown in this figure, with the increase of the pulse duration, though the start point of the continuum spectrum moves a little along the harmonic order axis, the end point of the continuum has almost no change, which indicates that our quantum control scheme for the generation of the ultrabroad supercontinuum spectrum (namely, the harmonics between the start and the end points) is also suitable for the chirped pulse with a longer duration (the laser pulse with a longer duration is much easier to achieve in experiment). In addition, we also find that the harmonic intensity will be multiplied several times when the duration of the chirped pulse changes from 10 fs to 20 fs. When the duration of the chirped pulse is less than 10 fs, the harmonic intensity and the spectral cutoff as well as the supercontinuum width will be decreased, especially for the case with the duration of $\tau_0 \leq 5$ fs. Figure 6(b) presents the generated harmonic spectra with five different intensities of the static electric field. From Fig. 6(b), we can clearly see that the harmonic spectrum is sensitive to the variation of the intensity of the static electric field. If the static field strength is relatively low, this leads to a harmonic spectrum with larger modulation and decreases the supercontinuum width. Contrarily, if the static field strength is relatively high, the spectral modulation becomes smaller, and the spectrum becomes smoother, but the width of the supercontinuum becomes shorter. We also find that the harmonic intensity will be reduced with the increasing static field strength. For the case of 6×10^{14} W/cm^2, the dependences of the supercontinuum on the two parameters are the same as those above. Therefore, in practical experiments with our scheme, a proper static field strength should be chosen.

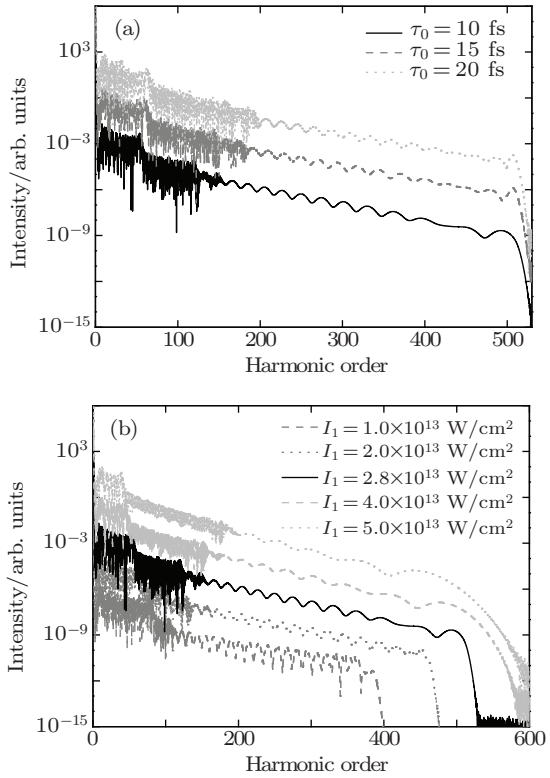


Fig. 6. (a) Harmonic spectra with three different durations of the 800-nm chirped pulse (the harmonic intensities for 15 fs and 20 fs are multiplied by the factors of 10^2 and 10^4, respectively). (b) Harmonic spectra with five different intensities of the static electric field (the harmonic intensities for 1.0×10^{13} W/cm^2, 2.0×10^{13} W/cm^2, 4.0×10^{13} W/cm^2, and 5.0×10^{13} W/cm^2 are multiplied by the factors of 10^{-4}, 10^{-2}, 10^2, and 10^4, respectively). The other parameters are the same as those in Fig. 1.

4. Conclusion

In conclusion, we have theoretically presented a method to generate an ultrabroad XUV supercontinuum using the combination of a multicycle 800-nm chirped pulse and a static electric field. It has been shown that this method can significantly modulate the quantum paths for the HHG. For the case of 4.0×10^{14} W/cm^2, the spectral cutoff is extended to the 495th order harmonic, and the bandwidth of the XUV supercontinuum spectrum is broadened to 535 eV. For the case of 6.0×10^{14} W/cm^2, the harmonic cutoff is enlarged to the 667th order, and a supercontinuum covering a bandwidth of 1035 eV is generated. In these two cases, due to the modulation of the static electric field, the long quantum path is removed, only the short one is selected to effectively contribute to the harmonic spectrum, and then an isolated ultrashort attosecond pulse can be obtained by filtering out some proper continuous harmonics. Especially with the relatively high laser intensity, we directly obtain an ultrashort isolated 23-as pulse with a bandwidth of 170.6 eV without any phase compensation. We also analyze the influence of the chirp parameter on the supercontinuum for the two different durations and investigate the dependence of the supercontinuum on the intensity of the static electric field. It is worthwhile to note that in this paper, the static field strength is extremely high and can hardly be achieved in experiment nowadays. However, it has been shown that a CO_2 laser field[25,37] or a strong terahertz field[38] can be used instead of the high static field. Our calculations also indicate that by applying a 100-μm THz field to the chirped pulse, similar results can be obtained. Such an effective controlling scheme can also use a combined field with a much longer duration, which makes our scheme more achievable in experiment. In short, the advantage of the scheme presented here lies in generating a broadband XUV supercontinuum in the multicycle regime, which is favorable for producing an ultrashort isolated attosecond pulse.

References

[1] Hentschel M, Kienberger R, Spielmann Ch, Reider G A, Milosevic N, Brabec T, Corkum P B, Heinzmann U, Drescher M and Krausz F 2001 *Nature* **414** 509

[2] Kienberger R, Goulielmakis E, Uiberacker M, Baltuska A, Yakovlev V, Bammer F, Scrinzi A, Westerwalbesloh T, Kleineberg U, Heinzmann U, Drescher M and Krausz F 2004 *Nature* **427** 817

[3] Sansone G, Benedetti E, Calegari F, Vozzi C, Avaldi L, Flammini R, Poletto L, Villoresi P, Altucci C, Velotta R, Stagira S, Silvestri S D and Nisoli M 2006 *Science* **314** 443

[4] Corkum P B 1993 *Phys. Rev. Lett.* **71** 1994

[5] Baltuška A, Udem T, Uiberacker M, Hentschel M, Goulielmakis E, Gohle C, Holzwarth R, Yakovlev V S, Scrinzi A, Hänsch T W and Krausz F 2003 *Nature* **421** 611

[6] Goulielmakis E, Schultze M, Hofstetter M, Yakovlev V S, Gagnon J, Uiberacker M, Aquila A L, Gullikson E M, Attwood D T, Kienberger R, Krausz F and Kleineberg U 2008 *Science* **320** 1614

[7] Zeng Z N, Cheng Y, Song X H, Li R X and Xu Z Z 2007 *Phys. Rev. Lett.* **98** 203901

[8] Lan P F, Lu P X, Cao W, Li Y H and Wang X L 2007 *Phys. Rev.* A **76** 011402(R)

[9] Lan P F, Lu P X, Cao W, Li Y H and Wang X L 2007 *Phys. Rev.* A **76** 051801(R)

[10] Song X H, Zeng Z N, Fu Y X, Cai B, Li R X, Cheng Y and Xu Z Z 2007 *Phys. Rev.* A **76** 043830

[11] Cao W, Lu P X, Lan P F, Hong W Y and Wang X L 2007 *J. Phys.* B **40** 869

[12] Hong W Y, Lu P X, Lan P F, Li Q G, Zhang Q B, Yang Z Y and Wang X B 2008 *Phys. Rev.* A **78** 063407

[13] Zhai Z and Liu X S 2008 *J. Phys.* B **41** 125602

[14] Luo L Y, Du H C and Hu B T 2012 *Chin. Phys.* B **21** 033202
[15] Schafer K J and Gaarde M B 2004 *Phys. Rev. Lett.* **92** 023003
[16] Lan P F, Lu P X, Cao W and Wang X L 2007 *Phys. Rev.* A **76** 043808
[17] Wang S Y, Hong W Y, Zhang Q B, Li Q G and Lu P X 2010 *Chin. Phys.* B **19** 083203
[18] Antoine P, L'Huillier A and Lewenstein M 1996 *Phys. Rev. Lett.* **77** 1234
[19] Gaarde M B, Antoine P, L'Huillier A, Schafer K J and Kulander K C 1998 *Phys. Rev.* A **57** 4553
[20] Lan P F, Lu P X, Li Q G, Li F, Hong W Y and Zhang Q B 2009 *Phys. Rev.* A **79** 043413
[21] Lan P F, Lu P X, Li F, Li Q G, Hong W Y, Zhang Q B, Yang Z Y and Wang X B 2008 *Opt. Express* **16** 17542
[22] Dai J, Zeng Z N, Li R X and Xu Z Z 2010 *Chin. Phys.* B **19** 113203
[23] Carrera J J and Chu S I 2007 *Phys. Rev.* A **75** 033807
[24] Wu J, Zhai Z and Liu X S 2010 *Chin. Phys.* B **19** 093201
[25] Xiang Y, Niu Y P and Gong S Q 2009 *Phys. Rev.* A **79** 053419
[26] Li P C, Zhou X X, Wang G L and Zhao Z X 2009 *Phys. Rev.* A **80** 053825
[27] Xu J J, Zeng B and Yu Y L 2010 *Phys. Rev.* A **82** 053822
[28] Feng L Q and Chu T S 2011 *Phys. Rev.* A **84** 053853
[29] Odžak S and Milošević D B 2005 *Phys. Rev.* A **72** 033407
[30] Wang B B, Li X F and Fu P M 1998 *J. Phys.* B **31** 1961
[31] Wang B B, Li X F and Fu P M 1999 *Phys. Rev.* A **59** 2894
[32] Hong W Y, Lu P X, Cao W, Lan P F and Wang X L 2007 *J. Phys.* B **40** 2321
[33] Zhang G T, Bai T T ang Zhang M G 2012 *Chin. Phys.* B **21** 054214
[34] Borca1 B, Flege A V, Frolov M V, Manakov N L, Milošević D B and Starace A F 2000 *Phys. Rev. Lett.* **85** 732
[35] Feit M D, Fleck Jr J A and Steiger A 1982 *J. Comput. Phys.* **47** 412
[36] Antoine P and Piraux B 1995 *Phys. Rev.* A **51** R1750
[37] Wang B B, Li X F and Fu P M 2000 *Phys. Rev.* A **62** 063816
[38] Hong W Y, Lu P X, Lan P F, Zhang Q B and Wang X B 2009 *Opt. Express* **17** 5139